(12) INTERNATIONAL APPLICATION PUBLISHED UNDER THE PATENT COOPERATION TREATY (PCT)

(19) World Intellectual Property Organization
International Bureau

(43) International Publication Date
19 July 2012 (19.07.2012)

WIPO | PCT

(10) International Publication Number
WO 2012/096847 A2

(51) International Patent Classification:
G03F 1/22 (2012.01) *G03F 1/24* (2012.01)

(21) International Application Number:
PCT/US2012/020504

(22) International Filing Date:
6 January 2012 (06.01.2012)

(25) Filing Language: English

(26) Publication Language: English

(30) Priority Data:
61/431,768 11 January 2011 (11.01.2011) US

(71) Applicant *(for all designated States except US)*: **KLA-TENCOR CORPORATION** [US/US]; 1 Technology Drive, Milpitas, California 95035 (US).

(72) Inventors; and

(75) Inventors/Applicants *(for US only)*: **WACK, Daniel, C.** [US/US]; 1930 Lundy Lane, Los Altos, California 94024 (US). **KVAMME, Damon, F.** [US/US]; 16816 Frank Avenue, Los Gatos, California 95032 (US). **ROGERS, John, R.** [US/US]; 404 W. Hillcrest Blvd., Monrovia, California 94016 (US). **MCGUIRE, James, P., Jr.** [US/US]; 1720 Kaweah Drive, Pasadena, California 91105 (US). **RODGERS, John, M.** [US/US]; 3280 East Foothill Blvd., Suite 300, Pasadena, California 91107 (US).

(74) Agent: **OKAMOTO, James K.**; Okamoto & Benedicto LLP, P.O. Box 641330, San Jose, California 95164-1330 (US).

(81) Designated States *(unless otherwise indicated, for every kind of national protection available)*: AE, AG, AL, AM, AO, AT, AU, AZ, BA, BB, BG, BH, BR, BW, BY, BZ, CA, CH, CL, CN, CO, CR, CU, CZ, DE, DK, DM, DO, DZ, EC, EE, EG, ES, FI, GB, GD, GE, GH, GM, GT, HN, HR, HU, ID, IL, IN, IS, JP, KE, KG, KM, KN, KP, KR, KZ, LA, LC, LK, LR, LS, LT, LU, LY, MA, MD, ME, MG, MK, MN, MW, MX, MY, MZ, NA, NG, NI, NO, NZ, OM, PE, PG, PH, PL, PT, QA, RO, RS, RU, RW, SC, SD, SE, SG, SK, SL, SM, ST, SV, SY, TH, TJ, TM, TN, TR, TT, TZ, UA, UG, US, UZ, VC, VN, ZA, ZM, ZW.

[Continued on next page]

(54) Title: APPARATUS FOR EUV IMAGING AND METHODS OF USING SAME

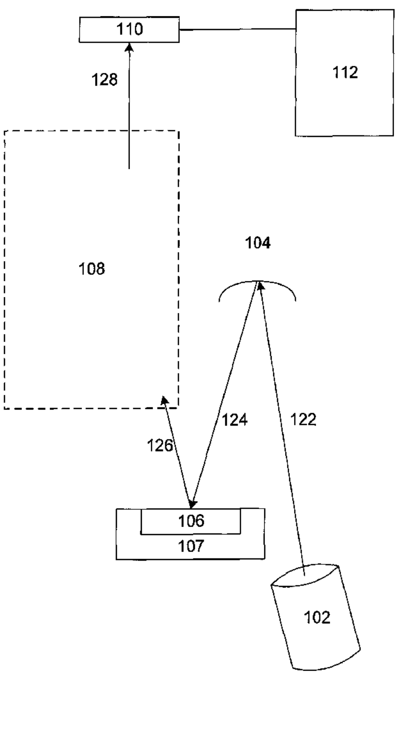

FIG. 1

(57) Abstract: One embodiment relates to an apparatus that includes an illumination source (102) for illuminating a target substrate (106), objective optics (108) for projecting the EUV light which is reflected from the target substrate, and a sensor (110) for detecting the projected EUV light. The objective optics includes a first mirror (202,302, or 402) which is arranged to receive and reflect the EUV light which is reflected from the target substrate, a second mirror (204, 304, or 404) which is arranged to receive and reflect the EUV light which is reflected by the first mirror, a third mirror (206, 306, or 406) which is arranged to receive and reflect the EUV light which is reflected by the second mirror, and a fourth mirror (208, 308, or 408) which is arranged to receive and reflect the EUV light which is reflected by the third mirror.

WO 2012/096847 A2

(84) Designated States *(unless otherwise indicated, for every kind of regional protection available)*: ARIPO (BW, GH, GM, KE, LR, LS, MW, MZ, NA, RW, SD, SL, SZ, TZ, UG, ZM, ZW), Eurasian (AM, AZ, BY, KG, KZ, MD, RU, TJ, TM), European (AL, AT, BE, BG, CH, CY, CZ, DE, DK, EE, ES, FI, FR, GB, GR, HR, HU, IE, IS, IT, LT, LU, LV, MC, MK, MT, NL, NO, PL, PT, RO, RS, SE, SI, SK, SM, TR), OAPI (BF, BJ, CF, CG, CI, CM, GA, GN, GQ, GW, ML, MR, NE, SN, TD, TG).

Published:

— *without international search report and to be republished upon receipt of that report (Rule 48.2(g))*

APPARATUS FOR EUV IMAGING AND METHODS OF USING SAME

Inventors:
Daniel C. Wack; Damon F. Kvamme; John R. Rogers; James P. McGuire, Jr.; and John M. Rodgers.

CROSS-REFERENCE TO RELATED APPLICATION(S)

The present application claims the benefit of U.S. provisional patent application number 61/431,768, entitled "Apparatus for EUV Imaging and Methods of Using Same," filed January 11, 2011, the disclosure of which is hereby incorporated by reference.

BACKGROUND OF THE INVENTION

TECHNICAL FIELD

The present disclosure relates to optical apparatus and methods of using same.

DESCRIPTION OF THE BACKGROUND ART

The conventional apparatus in the market for photomask inspection generally employ ultra-violet (UV) light with wavelengths at or above 193 nanometers (nm). This is suitable for masks designed for use in lithography based on 193nm light. To improve further the printing of minimum feature sizes, next generation lithographic equipment is now designed for operation in the neighborhood of 13.5nm. Accordingly, patterned masks designed for operation near 13nm must be inspected. Such masks are reflective, having a patterned absorber layer over a resonantly-reflecting substrate (EUV multilayer, typically 40 pairs of MoSi with a 7nm period. The conventional inspection apparatus uses optics with a combination of wavelength and numerical apertures (NA) that are not sufficient (i.e. too small) to resolve pattern features and pattern defects of interest (printable) in EUV mask patterns characterized by a half-pitch below 22 nanometers (nm).

SUMMARY

One embodiment disclosed relates to an apparatus for inspecting a photomask using extreme ultra-violet (EUV) light. The apparatus includes an illumination source for generating the EUV light which illuminates a target substrate, objective optics for receiving and projecting the EUV light which is reflected from the target substrate, and a sensor for detecting the EUV light which is projected by the objective optics. The objective optics includes a first mirror which is arranged to receive and reflect the EUV light which is reflected from the target substrate, a second mirror which is arranged to receive and reflect the EUV light which is reflected by the first mirror, a third mirror which is arranged to receive and reflect the EUV light which is reflected by the second mirror, and a fourth mirror which is arranged to receive and reflect the EUV light which is reflected by the third mirror.

Other embodiments, aspects and features are also disclosed.

BRIEF DESCRIPTION OF THE DRAWINGS

FIG. 1 is a schematic diagram of a reflective imaging apparatus in accordance with an embodiment of the invention.

FIG. 2 is an optical ray diagram of a mirror distribution for reflective objective optics in accordance with a first embodiment of the invention.

FIG. 3 is an optical ray diagram of a mirror distribution for reflective objective optics in accordance with a second embodiment of the invention.

FIG. 4 is an optical ray diagram of a mirror distribution for reflective objective optics in accordance with a third embodiment of the invention.

DETAILED DESCRIPTION

EUV microscope objectives (having 2 to 4 multilayer-coated mirrors) disclosed previously, designed for defect or pattern review applications, with operation in the neighborhood of 13nm wavelength of light, are based have NA in the range 0.05 – 0.12, and an object field extent just adequate to the review (microscopy) task – in the range of 5-20 microns at the mask. According to rigorous analyses of the defect detection capability as a function of NA and defect size, the resolving power and defect detection sensitivity of EUV objectives with NA in this range are inadequate for production-worthy EUV mask inspection of masks with feature half-pitch (HP) below 18 nm or so, due to shortcomings in both NA and high-quality object field size.

Current mask inspection systems are based on UV and DUV laser sources of light, which are high brightness and relatively high power. Light sources with significant spectral brightness in the neighborhood of 13nm are based on pulsed plasmas, with temperatures in the range 20-50 eV. Due to poor conversion efficiency (conversion from input energy to in-band radiation), such plasma sources show limited brightness at 13-14 nm, and raising the brightness significantly can drive source cost (and thus inspection costs imposed on the mask during fabrication) to levels which impair the economic attractiveness of EUV Lithography (EUVL).

High-throughput operation of mask inspection systems with low brightness plasma sources (discharge or laser produced) drives the need for large object field and detector array, to increase the rate of instantaneous image signal integration and conversion to digital representation.

Simultaneously, to discriminate defect signals from background image noise, the imaging optics must maximize the collection of light diffracted or scattered by patterning or multilayer defects residing on the EUV mask of interest. For most defects of interest, which diffract and scatter the incident light over a wide range of angles, increasing the NA of the objective will provide an increase in defect signals.

Multilayer-mirror based imaging systems have poor transmission of light, due to the limited reflectivity of multilayers at the design wavelengths near 13-14 nm. A single MoSi multilayer mirror shows peak spectral reflectivity near

13.5 nm in the range of 60-70%. After multiple reflections from near-normal incidence mirrors in typical illumination and imaging optics in an EUV system, system transmission can fall below 1%.

To perform the inspection task adequately, the light reaching the image plane and converted to digital signals by the detector array, from each resolved region of the mask, must reach a certain number of primary (13nm) quanta, and so a certain minimum signal-to-noise ratio, which in well designed systems is a strong function of the number of primary quanta (photons absorbed in the detector material, typically silicon). To compensate for losses in the optical system while keeping the light incident on the detector constant, the source brightness must be increased, which is difficult to develop and expensive to produce using currently known source technologies.

Alternatively, the range of angles emitted by the source which are transferred to the mask by the illumination optics can be increased, since the amount of light will increase with this angular range, at least within a range of angles supported by the source brightness. In other words, the illumination pupil size can be increased until a physical constraint intervenes. Rigorous studies of defect SNR in inspection optic designs have indicated that for EUV masks, such largely incoherent imaging often provides higher SNR than lower sigma, more coherent operation of the design and system, when used with plasma sources of limited brightness.

The use of beam splitters in reflective imaging systems used in conjunction with reflective objects (such as EUV mask inspection using EUV light) can simplify optical design and layout, by allowing interpenetration or overlap of illumination and imaging pupils in angle space. Current EUV beam splitter technology have low reflection and transmission coefficients (25-35 %). Inspection systems with beamsplitters must increase source brightness greatly to compensate for the loss of light reaching the detector. Inspection optics without a beamsplitter element is thus strongly preferred.

Light at wavelengths within the spectral bandpass of the resonantly-reflecting multilayer incident on such a uniform (unpatterned) mirror is reflected at 60-70% only if the angle of incidence resides within the angular bandpass as well. Periodic MoSi multilayers have an angular bandpass of 20-

25 degrees at 13.5nm. Light incident outside of the angular bandpass is reflected by the multilayer at very low levels, and thus is largely absorbed, or wasted.

Rigorous studies of light propagation and diffraction by patterns on EUV masks indicates that this trend holds for light incident on patterned masks, as well. Furthermore, the angular distribution of light diffracted and scattered by defects present on or in the EUV patterned mask is also modulated by the angular bandpass of the multilayer. The angular distribution of light scattered by a defect depends as well on the defect geometry, and the geometry of the local pattern, and can be significantly skewed to one side of the imaging pupil or another. To collect adequate light from all defect types and for arbitrary pattern geometries, the size of the imaging pupil should be maximized. Consequently, design of inspection optics without a beamsplitter and which operate largely within the finite angular bandwidth of the mask, and which utilize plasma sources of limited brightness, must contend with competing angular claims of the illumination and imaging pupils, each of which seek to maximize the size of their angular extent.

EUVL at 11HP may use aperiodic multilayers in the EUV mask design, which provide increased angular bandwidth, and enable EUVL imaging at higher NAs than possible with a conventional periodic multilayer design. This improves, but does not fully mitigate the issue of finite angular bandpass.

Although increasing the number of mirrors in an imaging design can provide design capability which enables simultaneous high NA and wide object field, this can lead to a prohibitive decrease in light reaching the detector. Thus, there is significant value in discovering designs which provide adequate inspection performance at minimum mirror count, which do not use a beam splitter, and which balance the competing needs of illuminating and imaging pupils sizes and locations, and thereby enable the production use of low brightness plasma-based EUV sources.

Furthermore, it is of strong economic interest to discover optical designs which provide adequate defect inspection performance for at least two technology nodes, for example 16HP and 11HP. As the critical defect size which limits chip yield shrinks with technology node, the NA of the inspection system should be increased to compensate for the reduction in scattered light.

In summary, conventional apparatus that utilize UV light are clearly limited when applied to inspect extreme ultra-violet photomasks ("EUV masks"). The conventional apparatus are typically "non-actinic" in that they result in an image of the mask that does not represent what will be realized using EUV light during lithography. Rather, the resultant image of the mask lacks both resolution and contrast, such that the image is not very useful for pattern inspection and defect detection.

More recently, photomask inspectors that use EUV light for imaging ("EUV inspectors") are being developed. However, the current EUV inspectors also have limitations and drawbacks. First, the field sizes of the images are very small. This limitation results in a low throughput when the apparatus is used to inspect entire EUV masks for defects. Second, numerical apertures of the optics are low. This limitation results in a relatively lower resolution. Such lower resolution limits the practical use of the images for pattern inspection and defect detection.

The present patent application discloses reflective imaging apparatus that overcome the above-discussed problems with photomask inspectors.

During inspection of patterned masks, acquisition and subsequent signal processing of the signal corresponding to a localized defective pattern can be accomplished by comparing or differencing the digital images from a test region of a pattern and a reference region, whether acquired or synthesized from prior information. Such difference operation removes the pattern, leaving the defect as a perturbation of a quasi-uniform background signal.

Imaging pupils are often circularly symmetric, leading to symmetric point spread functions at the image plane. While such symmetry is often required in lithography, mask inspection via difference imaging does not require symmetric psf, and consequently the imaging pupil can afford to be asymmetric. In particular, obscuration of a portion of the imaging pupil can be tolerated, if defect signal collection is not compromised significantly.

Additionally, the shape of the parent pupil need not be circular. For instance, square or rectangular shapes for the parent are possible, and even advantageous when considering the incremental gain of scattered defect light or signal through addition of pupil region.

Expressed as a fraction of pupil area, obscuration fractions less than 5 or 10% are preferred. Obscuration in 4-mirror designs is often created through the blocking or shadowing of light reflected or scattered from the mask by the second mirror, or M2. Minimizing the size of both reflecting surface and peripheral support of M2 will minimize obscuration.

The design of structural support for M2 must provide for sufficient rigidity, so that environmental disturbances or vibrations do not drive or lead to dynamic perturbations of M2 position and thus to degradation of image quality through blurring.

Since mirrors for EUV light must be coated with multilayers to reach adequate reflectivity, the range of incidence angles on any of the highly curved elements must be considered, and restricted within the limits of multilayer deposition process technology. When estimating the defect SNR of a particular objective and system design, the apodization or modulation of transmission of each light ray by local reflectivity variations at the point of reflection on each mirror induced by the multilayer deposition process must be considered.

In particular, the design process must balance obscuration, structural response and curvature factors in the geometry of the second mirror or M2, in order to secure the minimum viable defect SNR which enables fast and economic mask inspection.

The choice of chief ray in design of the objective for mask inspection must balance several competing factors. The chief ray is defined by the centroid of the angular distribution of light rays transmitted by the objective to the image plane; i.e., with due consideration of the pupil apodization caused by mirror coatings. Although conventional designs for reflective imaging without a beamsplitter place the plane dividing the illumination and collection light bundles on the optical axis and coincident with the object surface normal, inspection-oriented optics do not demand or strongly prefer this choice. Thus allowing placement of the lower marginal ray of the imaging pupil below the surface normal is found to be advantageous for defect signal collection.

Correspondingly, in the process of increasing defect SNR, as the NA is increased from low levels, in higher performance designs the imaging chief ray (relative to the surface normal) is below the numerical value of the NA. Inspection-optimized EUV objective designs bias the imaging chief rays toward the surface normal to maximize overlap of imaging pupil with multi-layer modulated angular distribution of light scattered by pattern defects, while providing sufficient angular range (still largely restricted to the multilayer angular bandpass) to the illumination pupil to secure adequate photon flux from the limited brightness plasma EUV sources.

FIG. 1 is a schematic diagram of a reflective imaging apparatus in accordance with an embodiment of the invention. The apparatus **100** includes an EUV illumination source **102**, an illumination mirror **104**, a target substrate **106**, a substrate holder **107**, objective optics **108**, a sensor (detector) **110**, and a data processing system **112**.

The EUV illumination source **102** may comprise, for example, a laser-induced plasma source which outputs an EUV light beam **122**. In one embodiment, the EUV light is at a wavelength of 13.5 nm. The illumination mirror **104** reflects the EUV light such that the beam **124** illuminates the target substrate **106**. In one embodiment of the invention, the target substrate **106** is an EUV mask being inspection. The target substrate **106** may be scanned under the beam **124** by controllably translating the substrate holder **107** so that the field of view of the imaging apparatus covers regions on the substrate to be inspected.

Patterned light **126** is reflected from the target substrate **106** to the reflective objective optics **108**. Preferred embodiments of the objective optics **108** are described in detail below in relation to FIGS. 2, 3 and 4.

The objective optics **108** outputs a projection **128** of the patterned light onto the sensor **110**. In one embodiment, the sensor **110** may be a time-delay integration detector array so that the data may be detected while the target substrate is being scanned (translated) under the beam **124**.

The data processing system **112** may include electronic circuitry, one or more microprocessors, data storage, memory and input and output devices. The data processing system **112** may be configured to receive and process data from the sensor **110**. In accordance with one embodiment, the data processing system **112** may process and analyze the detected data for pattern inspection and defect detection.

FIG. 2 is an optical ray diagram of a mirror distribution for the objective optics **108** in accordance with a first embodiment of the invention. An optical prescription for the objective optics **108** in FIG. 2 is provided below in Appendix A.

In this embodiment, there are four mirrors (**202**, **204**, **206**, and **208**) arranged as shown in FIG. 2. The mirrors are arranged such that the patterned light **126** reflects from the first, second, third, and fourth mirrors (**202**, **204**, **206**, and **208**, respectively) in that order. In this arrangement, the first mirror **202** is concave, the second mirror **204** is concave, the third mirror **206** is convex, the fourth mirror **208** is concave. Hence, the mirrors are, in order: concave; concave; convex; and concave.

In this embodiment, the second mirror **204** partially obscures the first mirror **202** from the patterned light **126**. In other words, part of the area of the first mirror **202** is blocked by the second mirror **204** from receiving the light **126** reflected from the target substrate **106**. Furthermore, an opening in the first mirror **202** is used to let the light reflected by the second mirror **204** pass through to reach the third mirror **206**. Applicants have determined that, despite the first mirror **202** being partially obscured and needing a pass-through hole, a high numerical aperture is nevertheless achieved with this embodiment.

In accordance with a preferred embodiment, the numerical aperture for the objective optics is at least 0.2, and the field of view is at least 5,000 square microns in area. For this implementation of the objective optics **108**, the numerical aperture has been determined to be 0.24, and the size of the field of view has been determined to be 327 microns by 30 microns (9,810 square microns in area). Advantageously, both the numerical aperture and field of view are relatively large in this embodiment.

The working distance is the distance between the target substrate **106** and the nearest optical element (in this case, the second mirror **204**). A working distance of at least 100 millimeters (mm) is desirable to provide sufficient space for illumination of the target substrate **106**. In this embodiment, the working distance is 145 mm.

The total track may be defined as the distance from the target substrate **106** to the sensor **110**. In this particular embodiment, the total trace is 1,500 mm.

FIG. 3 is an optical ray diagram of a mirror distribution for reflective objective optics in accordance with a second embodiment of the invention. An optical prescription for the objective optics **108** in FIG. 3 is provided below in Appendix B.

In this embodiment, there are four mirrors (**302**, **304**, **306**, and **308**) arranged as shown in FIG. 3. The mirrors are arranged such that the patterned light **126** reflects from the first, second, third, and fourth mirrors (**302**, **304**, **306**, and **308**, respectively) in that order. In this arrangement, the first mirror **302** is concave, the second mirror **304** is concave, the third mirror **306** is convex, the fourth mirror **308** is concave. Hence, the mirrors are, in order: concave; convex; concave; and convex.

In this embodiment, the second mirror **304** partially obscures the first mirror **302** from the patterned light **126**. In other words, part of the area of the first mirror **302** is blocked by the second mirror **304** from receiving the light **126** reflected from the target substrate **106**. Furthermore, an opening in the first mirror **302** is used to let the light reflected by the second mirror **304** pass through to reach the third mirror **306**. Applicants have determined that, despite the first mirror **302** being partially obscured and needing a pass-through hole, a high numerical aperture is nevertheless achieved with this embodiment.

In accordance with a preferred embodiment, the numerical aperture for the objective optics is at least 0.2, and the field of view is at least 5,000 square microns in area. For this implementation of the objective optics **108**, the numerical aperture has been determined to be 0.24, and the size of the field of view has been determined to be 440 microns by 420 microns (184,800 square microns in area). Advantageously, the numerical aperture is relatively large in this embodiment, and the field of view is particularly large. The large field of view advantageously enables multiple sensor columns.

The working distance is the distance between the target substrate **106** and the nearest optical element (in this case, the second mirror **304**). A working distance of at least 100 millimeters (mm) is desirable to provide sufficient space for illumination of the target substrate **106**. In this embodiment, the working distance is 237 mm.

The total track may be defined as the distance from the target substrate **106** to the sensor **110**. In this particular embodiment, the total trace is 873 mm.

FIG. 4 is an optical ray diagram of a mirror distribution for reflective objective optics in accordance with a third embodiment of the invention. An optical prescription for the objective optics **108** in FIG. 4 is provided below in Appendix C.

In this embodiment, there are four mirrors (**402**, **404**, **406**, and **408**) arranged as shown in FIG. 4. The mirrors are arranged such that the patterned light **126** reflects from the first, second, third, and fourth mirrors (**402**, **404**, **406**, and **408**, respectively) in that order. In this arrangement, the first mirror **402** is concave, the second mirror **404** is convex, the third mirror **406** is concave, the fourth mirror **408** is concave. Hence, the mirrors are, in order: concave; convex; concave; and concave.

In this embodiment, the second mirror **404** partially obscures the first mirror **402** from the patterned light **126**. In other words, part of the area of the first mirror **402** is blocked by the second mirror **404** from receiving the light **126** reflected from the target substrate **106**. Furthermore, an opening in the first mirror **402** is used to let the light reflected by the second mirror **404** pass through to reach the third mirror **406**. Applicants have determined that, despite the first mirror **402** being partially obscured and needing a pass-through hole, a high numerical aperture is nevertheless achieved with this embodiment.

In accordance with a preferred embodiment, the numerical aperture for the objective optics is at least 0.2, and the field of view is at least 5,000 square microns in area. For this implementation of the objective optics **108**, the numerical aperture has been determined to be 0.24, and the size of the field of view has been determined to be 410 microns by 255 microns (104,550 square microns in area). Advantageously, the numerical aperture is relatively large in this embodiment, and the field of view is also large.

The working distance is the distance between the target substrate **106** and the nearest optical element (in this case, the second mirror **404**). A working distance of at least 100 millimeters (mm) is desirable to provide sufficient space for illumination of the target substrate **106**. In this embodiment, the working distance is 230 mm.

The total track may be defined as the distance from the target substrate **106** to the sensor **110**. In this particular embodiment, the total trace is 1,420 mm.

In the above description, numerous specific details are given to provide a thorough understanding of embodiments of the invention. However, the above description of illustrated embodiments of the invention is not intended to be exhaustive or to limit the invention to the precise forms disclosed. One skilled in the relevant art will recognize that the invention can be practiced without one or more of the specific details, or with other methods, components, etc. In other instances, well-known structures or operations are not shown or described in detail to avoid obscuring aspects of the invention. While specific embodiments of, and examples for, the invention are described herein for illustrative purposes, various equivalent modifications are possible within the scope of the invention, as those skilled in the relevant art will recognize.

These modifications can be made to the invention in light of the above detailed description. The terms used in the following claims should not be construed to limit the invention to the specific embodiments disclosed in the specification and the claims. Rather, the scope of the invention is to be determined by the following claims, which are to be construed in accordance with established doctrines of claim interpretation.

APPENDIX A

Optical Prescription for Objective Optics depicted in FIG. 2.

Form: PPNP (type K)

ELT NO.	SUR NO.	SURFACE DESCRIPTION RADIUS X	RADIUS Y	SHAPE	THICKNESS OR SEPARATION	APERTURE DESCRIPTION DIMENSION X	DIMENSION Y	SHAPE	MATERIAL
OBJECT		INF		FLT	171.5840				
		DECENTER(1)							
					-31.2583	114.258		CIR	
					157.5932	93.435	93.435	C-1	
		DECENTER(2)							
	1				15.2460	152.732	152.685	C-2	(STOP)
		RETURN(2)							
1	2	-207.101		A-1	-167.7470	167.526	166.181	C-3	REFL
2	3	25.266		A-2	87.7476	14.523	14.282	C-4	REFL
					79.9994	13.380		CIR	
					223.0383	10.546		C-5	
					0.1102	5.454		CIR	
3	4	21.112		A-3	-113.1924	5.712	0.899	C-6	REFL
4	5	439.339		A-4	1076.8791	64.605	6.679	C-7	REFL
IMAGE		INF		FLT		293.920			

NOTES - Positive radius indicates the center of curvature is to the right
Negative radius indicates the center of curvature is to the left
- Dimensions are given in millimeters

- Thickness is axial distance to next surface

- Image diameter shown above is a paraxial value, it is not a ray traced value

APERTURE DATA

APERTURE	SHAPE	DIAMETER X	DIAMETER Y	DECENTER X	DECENTER Y	ROTATION
C- 1	CIRCLE	93.435				

	ELLIPS	(OBSC)	14.282	14.523	0.000	-2.136	0.0
	RECTANGLE	(OBSC)	14.523	42.846	0.000	-23.559	0.0
C- 2	ELLIPS		152.732	152.685	0.000	-0.029	0.0
C- 3	ELLIPS		167.526	166.181	0.000	24.513	0.0
	CIRCLE	(OBSC)	10.546	10.546	0.000	-1.495	0.0
C- 4	ELLIPS		14.523	14.282	0.000	-2.136	0.0
C- 5	CIRCLE		10.546	10.546	0.000	-1.495	0.0
C- 6	RECTANGLE		5.712	0.899	0.000	-0.619	0.0
C- 7	RECTANGLE		64.605	6.679	0.000	-6.786	0.0

ASPHERIC CONSTANTS

$$Z = \frac{(CURV)Y^{2}}{1 + (1-(1+K)(CURV)^{2}Y^{2})^{1/2}} + (A)Y^{4} + (B)Y^{6} + (C)Y^{8} + (D)Y^{10} + (E)Y^{12} + (F)Y^{14} + (G)Y^{16} + (H)Y^{18} + (J)Y^{20}$$

ASPHERIC	CURV	K / E	A / F	B / G	C / H	D / J
A- 1	-0.00482857	-0.092398	4.73666E-10	1.00934E-14	1.65866E-19	6.57843E-24
		0.00000E+00	0.00000E+00	0.00000E+00	0.00000E+00	0.00000E+00
A- 2	0.03957902	0.557074	-7.96262E-06	-1.22560E-08	-3.24562E-11	1.31052E-13
		-9.70137E-16	0.00000E+00	0.00000E+00	0.00000E+00	0.00000E+00
A- 3	0.04736557	-0.131506	-2.22840E-06	-9.90910E-09	2.45154E-10	0.00000E+00
		0.00000E+00	0.00000E+00	0.00000E+00	0.00000E+00	0.00000E+00
A- 4	0.00227615	0.000000	-4.22762E-09	0.00000E+00	0.00000E+00	0.00000E+00
		0.00000E+00	0.00000E+00	0.00000E+00	0.00000E+00	0.00000E+00

DECENTERING CONSTANTS

DECENTER	X	Y	Z	ALPHA	BETA	GAMMA

```
-------------------------------------------------------------------------------------------
D( 1)      0.0000        0.0377        0.0000      0.0000      0.0000
0.0000
D( 2)      0.0000        24.8300       0.0000      6.6732      0.0000
0.0000   (RETU)
```

A decenter defines a new coordinate system (displaced and/or rotated) in which subsequent surfaces are defined. Surfaces following a decenter are aligned on the local mechanical axis (z-axis) of the new coordinate system. The new mechanical axis remains in use until changed by another decenter. The order in which displacements and tilts are applied on a given surface is specified using different decenter types and these generate different new coordinate systems; those used here are explained below. Alpha, beta, and gamma are in degrees.

DECENTERING CONSTANT KEY:

TYPE	TRAILING CODE	ORDER OF APPLICATION
DECENTER		DISPLACE (X,Y,Z) TILT (ALPHA,BETA,GAMMA) REFRACT AT SURFACE THICKNESS TO NEXT SURFACE
DECENTER & RETURN	RETU	DECENTER (X,Y,Z,ALPHA,BETA,GAMMA) REFRACT AT SURFACE RETURN (-GAMMA,-BETA,-ALPHA,-Z,-Y,-X) THICKNESS TO NEXT SURFACE

```
-------------------------------------------------------------------------------------------

REFERENCE WAVELENGTH =        13.5 NM

-------------------------------------------------------------------------------------------
```

This is a non-symmetric system. If elements with power are decentered or tilted, the first order properties are probably inadequate in describing the system characteristics.

```
INFINITE CONJUGATES      X          Y
  EFL          =    -1.5852    -1.5852
  BFL          =  -281.8874  -281.8874
  FFL          =  -171.5821  -171.5821
  F/NO         =    -0.0107    -0.0107

AT USED CONJUGATES
  REDUCTION    =  -860.5581  -860.5581
  FINITE F/NO  = -1787.6352 -1776.3433
  OBJECT DIST  =   171.5840   171.5840
  TOTAL TRACK  =  1500.0000  1500.0000
  IMAGE DIST   =  1076.8791  1076.8791
  OAL          =   251.5370   251.5370
  PARAXIAL
    IMAGE HT   =   104.2136     1.0040
    IMAGE DIST =  1082.2952  1082.2952
  SEMI-FIELD
    ANGLE      =    80.1437     3.1738
  ENTR PUPIL
    DIAMETER   =   147.8187   148.7584
    DISTANCE   =   126.3350   126.3350
  EXIT PUPIL
    DIAMETER   =     0.7865     0.7915
    DISTANCE   =  -281.8958  -281.8958

-------------------------------------------------------------------------------------------

NOTES - FFL is measured from the first surface
      - BFL is measured from the last surface
```

PPNP_CaseK_120110

ASPHERIC CONSTANTS

$$Z = \frac{(CURV)Y^{2}}{1 + (1-(1+K)(CURV)^{2}Y^{2})^{1/2}} + (A)Y^{4} + (B)Y^{6} + (C)Y^{8} + (D)Y^{10}$$

ASPHERIC	CURV	K	A	B	C	D
A(1)	-0.00482857	-0.092398	0.473666E-09	0.100934E-13	0.165866E-18	0.657843E-23

CURVATURE OF BEST SPHERE = -0.004794
RADIUS OF BEST SPHERE = -208.591

Y	ASPH SAG (Z)	SPHERE SAG	SAG DIFFERENCE
0.000000	0.000000	0.000000	0.000000
3.857000	-0.035919	-0.035662	0.000256
7.714000	-0.143708	-0.142686	0.001021
11.571000	-0.323465	-0.321182	0.002283
15.428000	-0.575355	-0.571333	0.004022
19.285000	-0.899608	-0.893398	0.006209
23.142000	-1.296523	-1.287713	0.008810
26.999000	-1.766468	-1.754691	0.011777
30.856000	-2.309882	-2.294825	0.015057
34.713000	-2.927276	-2.908692	0.018584
38.570000	-3.619238	-3.596954	0.022284
42.427000	-4.386433	-4.360362	0.026070
46.284000	-5.229607	-5.199764	0.029843
50.141000	-6.149595	-6.116105	0.033490
53.998000	-7.147317	-7.110433	0.036884
57.855000	-8.223792	-8.183911	0.039881
61.712000	-9.380135	-9.337817	0.042318
65.569000	-10.617572	-10.573557	0.044015
69.426000	-11.937439	-11.892674	0.044765
73.283000	-13.341195	-13.296857	0.044339
77.140000	-14.830431	-14.787955	0.042477
80.997000	-16.406878	-16.367990	0.038887
84.854000	-18.072418	-18.039176	0.033241
88.711000	-19.829100	-19.803933	0.025167
92.568000	-21.679156	-21.664911	0.014246
96.425000	-23.625013	-23.625013	0.000000

PPNP_CaseK_120110

ASPHERIC CONSTANTS

$$Z = \frac{(CURV)Y^{2}}{1 + (1-(1+K)(CURV)^{2}Y^{2})^{1/2}} + (A)Y^{4} + (B)Y^{6} + (C)Y^{8} + (D)Y^{10} + (E)Y^{12} + (F)Y^{14} + (G)Y^{16} + (H)Y^{18} + (J)Y^{20}$$

ASPHERIC	CURV	K	A	B	C	D
		E	F	G	H	J
A(2)	0.03957902	0.557074	-0.796262E-05	-0.122560E-07	-0.324562E-10	0.131052E-12
		-0.970137E-15	0.000000E+00	0.000000E+00	0.000000E+00	0.000000E+00

CURVATURE OF BEST SPHERE = 0.039040
RADIUS OF BEST SPHERE = 25.615

Y	ASPH SAG (Z)	SPHERE SAG	SAG DIFFERENCE
0.000000	0.000000	0.000000	0.000000
0.332000	0.002181	0.002152	-0.000030
0.664000	0.008726	0.008608	-0.000118
0.996000	0.019636	0.019371	-0.000264
1.328000	0.034913	0.034448	-0.000465
1.660000	0.054563	0.053846	-0.000717
1.992000	0.078591	0.077574	-0.001017
2.324000	0.107003	0.105645	-0.001358
2.656000	0.139807	0.138073	-0.001734
2.988000	0.177013	0.174874	-0.002138
3.320000	0.218630	0.216068	-0.002562
3.652000	0.264671	0.261677	-0.002994
3.984000	0.315148	0.311723	-0.003425
4.316000	0.370076	0.366233	-0.003842
4.648000	0.429470	0.425237	-0.004232
4.980000	0.493348	0.488766	-0.004581
5.312000	0.561727	0.556855	-0.004873
5.644000	0.634629	0.629540	-0.005089
5.976000	0.712073	0.706862	-0.005212
6.308000	0.794084	0.788864	-0.005220
6.640000	0.880686	0.875593	-0.005092
6.972000	0.971904	0.967099	-0.004805
7.304000	1.067767	1.063435	-0.004332
7.636000	1.168304	1.164658	-0.003646
7.968000	1.273546	1.270829	-0.002717
8.300000	1.383527	1.382014	-0.001513
8.632000	1.498281	1.498281	0.000000

PPNP_CaseK_120110

ASPHERIC CONSTANTS

$$Z = \frac{(CURV)Y^2}{1 + (1-(1+K)(CURV)^2 Y^2)^{1/2}} + (A)Y^4 + (B)Y^6 + (C)Y^8 + (D)Y^{10}$$

ASPHERIC	CURV	K	A	B	C	D
A(3)	0.04736557	-0.131506	-0.222840E-05	-0.990910E-08	0.245154E-09	0.000000E+00

CURVATURE OF BEST SPHERE = 0.047274
RADIUS OF BEST SPHERE = 21.153

Y	ASPH SAG (Z)	SPHERE SAG	SAG DIFFERENCE
0.000000	0.000000	0.000000	0.000132
0.109000	0.000281	0.000281	0.000132
0.218000	0.001126	0.001123	0.000130
0.327000	0.002532	0.002528	0.000127
0.436000	0.004502	0.004494	0.000124
0.545000	0.007035	0.007022	0.000119
0.654000	0.010131	0.010112	0.000113
0.763000	0.013791	0.013765	0.000107
0.872000	0.018013	0.017981	0.000100
0.981000	0.022800	0.022760	0.000092
1.090000	0.028151	0.028102	0.000083
1.199000	0.034066	0.034008	0.000074
1.308000	0.040545	0.040478	0.000065
1.417000	0.047590	0.047514	0.000056
1.526000	0.055200	0.055115	0.000047
1.635000	0.063376	0.063282	0.000038
1.744000	0.072118	0.072015	0.000029
1.853000	0.081427	0.081316	0.000021
1.962000	0.091304	0.091186	0.000014
2.071000	0.101748	0.101624	0.000008
2.180000	0.112761	0.112632	0.000004
2.289000	0.124342	0.124211	0.000001
2.398000	0.136494	0.136362	0.000000
2.507000	0.149216	0.149085	0.000001
2.616000	0.162509	0.162382	0.000005
2.725000	0.176374	0.176254	0.000012

PPNP_CaseK_120110

ASPHERIC CONSTANTS

$$Z = \frac{(CURV)Y^{2}}{1 + (1-(1+K)(CURV)^{2}Y^{2})^{1/2}} + (A)Y^{4} + (B)Y^{6} + (C)Y^{8} + (D)Y^{10}$$

ASPHERIC	CURV	K	A	B	C	D
A(4)	0.00227615	0.000000	-0.422762E-08	0.000000E+00	0.000000E+00	0.000000E+00

CURVATURE OF BEST SPHERE = 0.002267
RADIUS OF BEST SPHERE = 441.054

Y	ASPH SAG (Z)	SPHERE SAG	SAG DIFFERENCE
0.000000	0.000000	0.000000	0.000000
1.247000	0.001770	0.001763	-0.000007
2.494000	0.007079	0.007051	-0.000027
3.741000	0.015927	0.015866	-0.000061
4.988000	0.028314	0.028206	-0.000108
6.235000	0.044239	0.044073	-0.000166
7.482000	0.063701	0.063466	-0.000235
8.729000	0.086700	0.086387	-0.000313
9.976000	0.113234	0.112836	-0.000399
11.223000	0.143303	0.142812	-0.000491
12.470000	0.176905	0.176318	-0.000586
13.717000	0.214038	0.213354	-0.000684
14.964000	0.254701	0.253921	-0.000780

16.211000	0.298891	0.298019	-0.000872
17.458000	0.346608	0.345650	-0.000958
18.705000	0.397849	0.396815	-0.001033
19.952000	0.452611	0.451516	-0.001095
21.199000	0.510891	0.509753	-0.001139
22.446000	0.572689	0.571528	-0.001161
23.693000	0.638000	0.636842	-0.001158
24.940000	0.706821	0.705697	-0.001124
26.187000	0.779150	0.778095	-0.001055
27.434000	0.854983	0.854037	-0.000946
28.681000	0.934317	0.933526	-0.000792
29.928000	1.017149	1.016562	-0.000586
31.175000	1.103474	1.103149	-0.000325
32.422000	1.193288	1.193288	0.000000

APPENDIX B

Optical Prescription for Objective Optics depicted in FIG. 3.

Form: PNPN (type E)

ELT NO.	SUR NO.	SURFACE DESCRIPTION RADIUS X	RADIUS Y	SHAPE	THICKNESS OR SEPARATION	APERTURE DESCRIPTION DIMENSION X	DIMENSION Y	SHAPE	MATERIAL
OBJECT		INF		FLT	231.9676				
					130.9218	161.906	161.906	C-1	
1	1	-202.870 (STOP)		A-1	-125.7510	168.744		C-2	REFL
2	2	-30.857		A-2	125.7510	20.585	20.683	C-3	REFL
					483.2695	22.288		CIR	
					1.9055	11.572		CIR	
3	3	-36.145		A-3	0.0000	7.765	5.068	C-4	REFL
		DECENTER(1)							
					100.0000	291.037		CIR	
4	4	2247.520	CC	SPH	0.0000	142.734	89.218	C-5	REFL
		DECENTER(2)							
					572.8054	382.502		CIR	
IMAGE		INF		FLT		615.460			

NOTES - Positive radius indicates the center of curvature is to the right
Negative radius indicates the center of curvature is to the left
- Dimensions are given in millimeters
- Thickness is axial distance to next surface
- Image diameter shown above is a paraxial value, it is not a ray traced value

APERTURE DATA

APERTURE	SHAPE		DIAMETER X	DIAMETER Y	DECENTER X	DECENTER Y	ROTATION
C- 1	CIRCLE		161.906				
	ELLIPS	(OBSC)	22.643	22.752	0.000	-3.554	0.0

	RECTANGLE	(OBSC)	20.585	76.760	0.000	34.826	0.0
C- 2	CIRCLE		168.744	168.744	0.000	-30.154	0.0
C- 3	ELLIPS		20.585	20.683	0.000	-3.554	0.0
C- 4	RECTANGLE		7.765	5.068	0.000	-2.531	0.0
C- 5	RECTANGLE		142.734	89.218	0.000	52.791	0.0

ASPHERIC CONSTANTS

$$Z = \frac{(CURV)Y^{2}}{1 + (1-(1+K)(CURV)^{2}Y^{2})^{1/2}} + (A)Y^{4} + (B)Y^{6} + (C)Y^{8} + (D)Y^{10}$$

ASPHERIC	CURV	K	A	B	C	D
A- 1	-0.00492927	-0.180985	0.00000E+00	-1.59047E-16	-3.25151E-21	-1.95259E-25
A- 2	-0.03240743	-0.742876	0.00000E+00	-8.96537E-11	-3.90040E-14	0.00000E+00
A- 3	-0.02766624	-4.312119	-8.98165E-06	9.34802E-09	0.00000E+00	0.00000E+00

DECENTERING CONSTANTS

DECENTER	X	Y	Z	ALPHA	BETA	GAMMA
D(1)	0.0000	0.0000	-485.1750	0.0000	0.0000	0.0000
D(2)	0.0000	0.0000	385.1750	0.0000	0.0000	0.0000

A decenter defines a new coordinate system (displaced and/or rotated) in which subsequent surfaces are defined. Surfaces following a decenter are aligned on the local mechanical axis (z-axis) of the new coordinate system. The new mechanical axis remains in use until changed by another decenter. The order in which displacements and tilts are applied on a given surface is specified using different decenter types and these generate different new coordinate systems; those used here are explained below. Alpha, beta, and gamma are in degrees.

DECENTERING CONSTANT KEY:

TYPE	TRAILING CODE	ORDER OF APPLICATION
DECENTER		DISPLACE (X,Y,Z) TILT (ALPHA,BETA,GAMMA) REFRACT AT SURFACE THICKNESS TO NEXT SURFACE

REFERENCE WAVELENGTH = 13.5 NM

This is a non-symmetric system. If elements with power are decentered or tilted, the first order properties are probably inadequate in describing the system characteristics.

```
INFINITE CONJUGATES
  EFL          =    -1.7535
  BFL          =  -929.1867
  FFL          =  -231.9655
  F/NO         =    -0.0069

AT USED CONJUGATES
  REDUCTION    =  -856.6454
  FINITE F/NO  = -1291.5539
  OBJECT DIST  =   231.9676
  TOTAL TRACK  =  1420.8698
  IMAGE DIST   =   572.8054
  OAL          =   616.0968
  PARAXIAL
    IMAGE HT   =   252.7104
    IMAGE DIST =   572.9594
  SEMI-FIELD
    ANGLE      =     0.0466
  ENTR PUPIL
    DIAMETER   =   255.1309
    DISTANCE   =   130.9218
  EXIT PUPIL
    DIAMETER   =     1.2328
    DISTANCE   =  -929.1951
```

NOTES - FFL is measured from the first surface
- BFL is measured from the last surface

----

schwarschild_4m857x_n.len

ASPHERIC CONSTANTS

$$Z = \frac{(CURV)Y^2}{1 + (1-(1+K)(CURV)^2 Y^2)^{1/2}} + (A)Y^4 + (B)Y^6 + (C)Y^8 + (D)Y^{10}$$

ASPHERIC	CURV	K	A	B	C	D
A(1)	-0.00492927	-0.180985	0.000000E+00	-0.159047E-15	-0.325151E-20	-0.195259E-24

CURVATURE OF BEST SPHERE = -0.004847
RADIUS OF BEST SPHERE = -206.293

Y	ASPH SAG (Z)	SPHERE SAG	SAG DIFFERENCE

0.000000	0.000000	0.000000	0.000000
4.581000	-0.051727	-0.050870	0.000857
9.162000	-0.206973	-0.203555	0.003419
13.743000	-0.465934	-0.458281	0.007652
18.324000	-0.828934	-0.815429	0.013505
22.905000	-1.296435	-1.275533	0.020903
27.486000	-1.869033	-1.839288	0.029745
32.067000	-2.547463	-2.507555	0.039908
36.648000	-3.332608	-3.281366	0.051242
41.229000	-4.225500	-4.161933	0.063567
45.810000	-5.227329	-5.150658	0.076672
50.391000	-6.339452	-6.249144	0.090308
54.972000	-7.563402	-7.459211	0.104191
59.553000	-8.900898	-8.782910	0.117988
64.134000	-10.353861	-10.222542	0.131319
68.715000	-11.924425	-11.780682	0.143743
73.296000	-13.614959	-13.460201	0.154758
77.877000	-15.428082	-15.264302	0.163780
82.458000	-17.366692	-17.196550	0.170142
87.039000	-19.433986	-19.260917	0.173069
91.620000	-21.633496	-21.461829	0.171667
96.201000	-23.969125	-23.804228	0.164897
100.782000	-26.445185	-26.293636	0.151549
105.363000	-29.066452	-28.936245	0.130207
109.944000	-31.838218	-31.739010	0.099208
114.525000	-34.766367	-34.709782	0.056584
119.106000	-37.857450	-37.857450	0.000000

schwarschild_4m857x_n.len

ASPHERIC CONSTANTS

$$Z = \frac{(CURV)Y^{2}}{1 + (1-(1+K)(CURV)^{2}Y^{2})^{1/2}} + (A)Y^{4} + (B)Y^{6} + (C)Y^{8} + (D)Y^{10}$$

ASPHERIC	CURV	K	A	B	C	D
A(2)	-0.03240743	-0.742876	0.000000E+00	-0.896537E-10	-0.390040E-13	0.000000E+00

CURVATURE OF BEST SPHERE = -0.031374
RADIUS OF BEST SPHERE = -31.873

Y	ASPH SAG (Z)	SPHERE SAG	SAG DIFFERENCE
0.000000	0.000000	0.000000	-0.022846
0.518000	-0.004348	-0.004209	-0.022707
1.036000	-0.017393	-0.016841	-0.022294
1.554000	-0.039137	-0.037906	-0.021614
2.072000	-0.069586	-0.067419	-0.020679
2.590000	-0.108745	-0.105405	-0.019505
3.108000	-0.156625	-0.151894	-0.018115
3.626000	-0.213234	-0.206924	-0.016535
4.144000	-0.278586	-0.270538	-0.014798
4.662000	-0.352695	-0.342790	-0.012941
5.180000	-0.435577	-0.423739	-0.011008
5.698000	-0.527251	-0.513451	-0.009046
6.216000	-0.627737	-0.612003	-0.007112
6.734000	-0.737058	-0.719479	-0.005267

7.252000	-0.855238	-0.835970	-0.003578
7.770000	-0.982306	-0.961580	-0.002120
8.288000	-1.118289	-1.096419	-0.000976
8.806000	-1.263219	-1.240609	-0.000236
9.324000	-1.417130	-1.394284	0.000000
9.842000	-1.580058	-1.557587	-0.000375
10.360000	-1.752042	-1.730675	-0.001479
10.878000	-1.933123	-1.913718	-0.003440
11.396000	-2.123346	-2.106899	-0.006399
11.914000	-2.322756	-2.310416	-0.010506
12.432000	-2.531403	-2.524486	-0.015928
12.950000	-2.749340	-2.749340	-0.022846

---

schwarschild_4m857x_n.len

ASPHERIC CONSTANTS

$$Z = \frac{(CURV)Y^2}{1 + (1-(1+K)(CURV)^2 Y^2)^{1/2}} + (A)Y^4 + (B)Y^6 + (C)Y^8 + (D)Y^{10}$$

ASPHERIC	CURV	K	A	B	C	D
A(3)	-0.02766624	-4.312119	-0.898165E-05	0.934802E-08	0.000000E+00	0.000000E+00

CURVATURE OF BEST SPHERE = -0.027493
RADIUS OF BEST SPHERE = -36.373

Y	ASPH SAG (Z)	SPHERE SAG	SAG DIFFERENCE
0.000000	0.000000	0.000000	0.000000
0.232000	-0.000745	-0.000740	0.000005
0.464000	-0.002978	-0.002960	0.000019
0.696000	-0.006701	-0.006660	0.000041
0.928000	-0.011913	-0.011840	0.000073
1.160000	-0.018614	-0.018502	0.000112
1.392000	-0.026805	-0.026646	0.000159
1.624000	-0.036485	-0.036273	0.000212
1.856000	-0.047654	-0.047384	0.000270
2.088000	-0.060313	-0.059981	0.000332
2.320000	-0.074462	-0.074065	0.000397
2.552000	-0.090101	-0.089638	0.000462
2.784000	-0.107229	-0.106702	0.000528
3.016000	-0.125849	-0.125258	0.000590
3.248000	-0.145958	-0.145310	0.000648
3.480000	-0.167559	-0.166860	0.000699
3.712000	-0.190651	-0.189910	0.000741
3.944000	-0.215234	-0.214463	0.000771
4.176000	-0.241308	-0.240522	0.000786
4.408000	-0.268875	-0.268091	0.000784
4.640000	-0.297935	-0.297173	0.000762
4.872000	-0.328487	-0.327772	0.000715
5.104000	-0.360533	-0.359891	0.000642
5.336000	-0.394073	-0.393535	0.000537
5.568000	-0.429106	-0.428708	0.000398
5.800000	-0.465635	-0.465414	0.000221
6.032000	-0.503658	-0.503658	0.000000

APPENDIX C

Optical Prescription for Objective Optics depicted in FIG. 4.

Form: PNPP (type B)

ELT NO.	SUR NO.	SURFACE DESCRIPTION RADIUS X	Y	SHAPE	THICKNESS OR SEPARATION	APERTURE DESCRIPTION DIMENSION X	Y	SHAPE	MATERIAL
OBJECT		INF		FLT	237.1340				
					125.5236	160.444		C-1	
		DECENTER(1)							
	1				0.0000	181.301		CIR	(STOP)
		RETURN(1)							
		DECENTER(2)							
1	2	-203.104		A-1	-125.5566	224.000		CIR	REFL
2	3	-31.766		A-2	420.3885	19.500		C-2	REFL
		DECENTER(3)							
3	4	INF		A-3	-224.8319	11.000	9.200	C-3	REFL
		RETURN(3)							
		DECENTER(4)							
4	5	35.266		A-4	985.5318	7.400	4.800	C-4	REFL
		RETURN(4)							
		DECENTER(5)							
IMAGE		INF		FLT		413.863			
		RETURN(5)							

NOTES - Positive radius indicates the center of curvature is to the right
Negative radius indicates the center of curvature is to the left
- Dimensions are given in millimeters
- Thickness is axial distance to next surface
- Image diameter shown above is a paraxial value, it is not a ray traced value

APERTURE DATA

APERTURE	SHAPE	DIAMETER X	Y	DECENTER X	Y	ROTATION
C- 1	CIRCLE	160.444				

		CIRCLE	(OBSC)	22.500	22.500	0.000	-3.175
0.0							
		RECTANGLE	(OBSC)	21.600	60.000	0.000	30.000
0.0							
	C- 2	CIRCLE		19.500	19.500	0.000	-3.175
0.0							
	C- 3	RECTANGLE		11.000	9.200	0.000	0.775
0.0							
	C- 4	RECTANGLE		7.400	4.800	0.000	2.920
0.0							

ASPHERIC CONSTANTS

$$Z = \frac{(CURV)Y^2}{1 + (1-(1+K)(CURV)^2 Y^2)^{1/2}} + (A)Y^4 + (B)Y^6 + (C)Y^8 + (D)Y^{10}$$

ASPHERIC	CURV	K	A	B	C	D
A- 1	-0.00492359	-0.177909	1.06780E-11	8.01201E-17	0.00000E+00	0.00000E+00
A- 2	-0.03147977	-0.645495	2.53860E-07	0.00000E+00	0.00000E+00	0.00000E+00
A- 3	0.00000000	0.000000	-8.75795E-08	0.00000E+00	0.00000E+00	0.00000E+00
A- 4	0.02835567	0.761823	-9.57017E-06	0.00000E+00	0.00000E+00	0.00000E+00

DECENTERING CONSTANTS

DECENTER	X	Y	Z	ALPHA	BETA	GAMMA	
D(1)	0.0000	-31.9686	0.0000	0.0000	0.0000	0.0000	(RETU)
D(2)	0.0000	0.2258	0.0000	0.0085	0.0000	0.0000	
D(3)	0.0000	0.0000	0.0000	3.6902	0.0000	0.0000	(RETU)
D(4)	0.0000	-29.1446	0.0000	7.3804	0.0000	0.0000	(RETU)
D(5)	0.0000	-51.4026	0.0000	7.3773	0.0000	0.0000	(RETU)

A decenter defines a new coordinate system (displaced and/or rotated) in which subsequent surfaces are defined. Surfaces following a decenter are aligned on the local mechanical axis (z-axis) of the new coordinate system. The new mechanical axis remains in use until changed by another decenter. The order in which displacements and tilts are applied on a given surface is specified using different decenter types and these generate different new coordinate systems; those used here are explained below. Alpha, beta, and gamma are in degrees.

DECENTERING CONSTANT KEY:

```
      TYPE               TRAILING CODE          ORDER OF APPLICATION
   ------------------------------------------------------------------------------

   DECENTER                                     DISPLACE (X,Y,Z)
                                                TILT (ALPHA,BETA,GAMMA)
                                                REFRACT AT SURFACE
                                                THICKNESS TO NEXT SURFACE

   DECENTER & RETURN      RETU                  DECENTER (X,Y,Z,ALPHA,BETA,GAMMA)
                                                REFRACT AT SURFACE
                                                RETURN (-GAMMA,-BETA,-ALPHA,-Z,-Y,-X)
                                                THICKNESS TO NEXT SURFACE

 -----------------------------------------------------------------------------------
-------------

 REFERENCE WAVELENGTH =         13.5 NM

 -----------------------------------------------------------------------------------
-------------

     This is a non-symmetric system.  If elements with power are
     decentered or tilted, the first order properties are probably
     inadequate in describing the system characteristics.

   INFINITE CONJUGATES
     EFL          =    -1.1191
     BFL          =    18.1212
     FFL          =  -237.1402
     F/NO         =    -0.0062

   AT USED CONJUGATES
     REDUCTION    =   179.1972
     FINITE F/NO  =   369.4788
     OBJECT DIST  =   237.1340
     TOTAL TRACK  =  1418.1894
     IMAGE DIST   =   985.5318
     OAL          =   195.5236
     PARAXIAL
       IMAGE HT   =    22.8476
       IMAGE DIST =  -182.4227
     SEMI-FIELD
       ANGLE      =     5.0067
     ENTR PUPIL
       DIAMETER   =   181.3005
       DISTANCE   =   125.5236
     EXIT PUPIL
       DIAMETER   =     0.5595
       DISTANCE   =    18.1177

 -----------------------------------------------------------------------------------
-------------

 NOTES - FFL is measured from the first surface
       - BFL is measured from the last surface

 -----------------------------------------------------------------------------------
---------

     RelayB_Dec032010.len

 -----------------------------------------------------------------------------------
-------------

 ASPHERIC CONSTANTS
```

$$Z = \frac{(CURV)Y^2}{1 + (1-(1+K)(CURV)^2 Y^2)^{1/2}} + (A)Y^4 + (B)Y^6 + (C)Y^8 + (D)Y^{10}$$

ASPHERIC	CURV	K	A	B	C	D

A(1)	-0.00492359	-0.177909	0.106780E-10	0.801201E-16	0.000000E+00	0.000000E+00

CURVATURE OF BEST SPHERE = -0.004853
RADIUS OF BEST SPHERE = -206.058

Y	ASPH SAG (Z)	SPHERE SAG	SAG DIFFERENCE
0.000000	0.000000	0.000000	0.000000
4.480000	-0.049414	-0.048707	0.000707
8.960000	-0.197716	-0.194896	0.002820
13.440000	-0.445083	-0.438775	0.006308
17.920000	-0.791815	-0.780693	0.011121
22.400000	-1.238330	-1.221141	0.017189
26.880000	-1.785174	-1.760755	0.024419
31.360000	-2.433019	-2.400325	0.032695
35.840000	-3.182670	-3.140794	0.041875
40.320000	-4.035066	-3.983273	0.051793
44.800000	-4.991294	-4.929043	0.062251
49.280000	-6.052588	-5.979570	0.073018
53.760000	-7.220341	-7.136511	0.083830
58.240000	-8.496116	-8.401738	0.094379
62.720000	-9.881655	-9.777342	0.104313
67.200000	-11.378892	-11.265663	0.113228
71.680000	-12.989969	-12.869307	0.120662
76.160000	-14.717253	-14.591169	0.126084
80.640000	-16.563355	-16.434472	0.128883
85.120000	-18.531152	-18.402793	0.128359
89.600000	-20.623816	-20.500111	0.123705
94.080000	-22.844840	-22.730853	0.113988
98.560000	-25.198079	-25.099953	0.098126
103.040000	-27.687786	-27.612923	0.074863
107.520000	-30.318661	-30.275932	0.042729
112.000000	-33.095910	-33.095910	0.000000

RelayB_Dec032010.len

ASPHERIC CONSTANTS

$$Z = \frac{(CURV)Y^2}{1 + (1-(1+K)(CURV)^2 Y^2)^{1/2}} + (A)Y^4 + (B)Y^6 + (C)Y^8 + (D)Y^{10}$$

ASPHERIC	CURV	K	A	B	C	D
A(2)	-0.03147977	-0.645495	0.253860E-06	0.000000E+00	0.000000E+00	0.000000E+00

CURVATURE OF BEST SPHERE = -0.030591
RADIUS OF BEST SPHERE = -32.689

Y	ASPH SAG (Z)	SPHERE SAG	SAG DIFFERENCE
0.000000	0.000000	0.000000	-0.019144
0.512000	-0.004126	-0.004010	-0.019027
1.024000	-0.016506	-0.016042	-0.018680

1.536000	-0.037141	-0.036107	-0.018109
2.048000	-0.066038	-0.064217	-0.017323
2.560000	-0.103201	-0.100395	-0.016337
3.072000	-0.148641	-0.144666	-0.015169
3.584000	-0.202366	-0.197065	-0.013843
4.096000	-0.264390	-0.257631	-0.012384
4.608000	-0.334727	-0.326409	-0.010826
5.120000	-0.413392	-0.403452	-0.009204
5.632000	-0.500403	-0.488819	-0.007559
6.144000	-0.595782	-0.582576	-0.005938
6.656000	-0.699550	-0.684798	-0.004392
7.168000	-0.811731	-0.795566	-0.002979
7.680000	-0.932353	-0.914969	-0.001760
8.192000	-1.061443	-1.043105	-0.000806
8.704000	-1.199032	-1.180080	-0.000192
9.216000	-1.345154	-1.326011	0.000000
9.728000	-1.499845	-1.481022	-0.000321
10.240000	-1.663142	-1.645250	-0.001253
10.752000	-1.835085	-1.818843	-0.002901
11.264000	-2.015718	-2.001958	-0.005384
11.776000	-2.205086	-2.194767	-0.008825
12.288000	-2.403238	-2.397456	-0.013362
12.800000	-2.610224	-2.610224	-0.019144

RelayB_Dec032010.len

ASPHERIC CONSTANTS

$$Z = \frac{(CURV)Y^{2}}{1 + (1-(1+K)(CURV)^{2}Y^{2})^{1/2}} + (A)Y^{4} + (B)Y^{6} + (C)Y^{8} + (D)Y^{10}$$

ASPHERIC	CURV	K	A	B	C	D
A(3)	0.00000000	0.000000	-0.875795E-07	0.000000E+00	0.000000E+00	0.000000E+00

CURVATURE OF BEST SPHERE = -0.000006
RADIUS OF BEST SPHERE = -171184.091

Y	ASPH SAG (Z)	SPHERE SAG	SAG DIFFERENCE
0.000000	0.000000	0.000000	0.000024
0.231000	0.000000	0.000000	0.000024
0.462000	0.000000	-0.000001	0.000024
0.693000	0.000000	-0.000001	0.000023
0.924000	0.000000	-0.000002	0.000022
1.155000	0.000000	-0.000004	0.000021
1.386000	0.000000	-0.000006	0.000019
1.617000	-0.000001	-0.000008	0.000017
1.848000	-0.000001	-0.000010	0.000015
2.079000	-0.000002	-0.000013	0.000013
2.310000	-0.000002	-0.000016	0.000011
2.541000	-0.000004	-0.000019	0.000009
2.772000	-0.000005	-0.000022	0.000007
3.003000	-0.000007	-0.000026	0.000005
3.234000	-0.000010	-0.000031	0.000003
3.465000	-0.000013	-0.000035	0.000002
3.696000	-0.000016	-0.000040	0.000001
3.927000	-0.000021	-0.000045	0.000000
4.158000	-0.000026	-0.000050	0.000000
4.389000	-0.000032	-0.000056	0.000001

4.620000	-0.000040	-0.000062	0.000002
4.851000	-0.000048	-0.000069	0.000004
5.082000	-0.000058	-0.000075	0.000007
5.313000	-0.000070	-0.000082	0.000012
5.544000	-0.000083	-0.000090	0.000017
5.775000	-0.000097	-0.000097	0.000024

RelayB_Dec032010.len

ASPHERIC CONSTANTS

$$Z = \frac{(CURV)Y^2}{1 + (1-(1+K)(CURV)^2 Y^2)^{1/2}} + (A)Y^4 + (B)Y^6 + (C)Y^8 + (D)Y^{10}$$

ASPHERIC	CURV	K	A	B	C	D
A(4)	0.02835567	0.761823	-0.957017E-05	0.000000E+00	0.000000E+00	0.000000E+00

CURVATURE OF BEST SPHERE = 0.027759
RADIUS OF BEST SPHERE = 36.024

Y	ASPH SAG (Z)	SPHERE SAG	SAG DIFFERENCE
0.000000	0.000000	0.000000	0.000000
0.249000	0.000879	0.000861	-0.000018
0.498000	0.003516	0.003442	-0.000073
0.747000	0.007910	0.007746	-0.000164
0.996000	0.014060	0.013772	-0.000289
1.245000	0.021965	0.021520	-0.000445
1.494000	0.031623	0.030993	-0.000629
1.743000	0.043031	0.042192	-0.000839
1.992000	0.056187	0.055118	-0.001069
2.241000	0.071088	0.069773	-0.001315
2.490000	0.087730	0.086159	-0.001571
2.739000	0.106109	0.104278	-0.001831
2.988000	0.126222	0.124134	-0.002087
3.237000	0.148062	0.145729	-0.002333
3.486000	0.171626	0.169066	-0.002560
3.735000	0.196908	0.194149	-0.002760
3.984000	0.223903	0.220981	-0.002922
4.233000	0.252603	0.249566	-0.003037
4.482000	0.283003	0.279908	-0.003094
4.731000	0.315095	0.312013	-0.003083
4.980000	0.348873	0.345884	-0.002990
5.229000	0.384330	0.381526	-0.002804
5.478000	0.421458	0.418946	-0.002511
5.727000	0.460248	0.458148	-0.002099
5.976000	0.500692	0.499139	-0.001553
6.225000	0.542783	0.541925	-0.000858
6.474000	0.586512	0.586512	0.000000

CLAIMS

What is claimed is:

1. An apparatus for inspecting a photomask using extreme ultra-violet (EUV) light, the apparatus comprising:

an illumination source for generating the EUV light which illuminates a target substrate;

objective optics for receiving and projecting the EUV light which is reflected from the target substrate; and

a sensor for detecting the EUV light which is projected by the objective optics,

wherein the objective optics comprises

a first mirror which is arranged to receive and reflect the EUV light which is reflected from the target substrate,

a second mirror which is arranged to receive and reflect the EUV light which is reflected by the first mirror,

a third mirror which is arranged to receive and reflect the EUV light which is reflected by the second mirror, and

a fourth mirror which is arranged to receive and reflect the EUV light which is reflected by the third mirror.

2. The apparatus of claim 1, wherein the second mirror partially obscures the first mirror from the reflected EUV light.

3. The apparatus of claim 1, wherein the light reflected by the second mirror passes through an opening in the first mirror.

4. The apparatus of claim 1, wherein the first, second, third, and fourth mirrors are, respectively, concave, concave, convex and concave.

5. The apparatus of claim 1, wherein the first, second, third, and fourth mirrors are, respectively, concave, convex, concave and convex.

6. The apparatus of claim 1, wherein the first, second, third, and fourth mirrors are, respectively, concave, convex, concave, and concave

7. The apparatus of claim 1, wherein the numerical aperture of the objective optics is greater than 0.2.

8. The apparatus of claim 1, wherein a field of view of the apparatus is at least greater than 5,000 square microns.

9. The apparatus of claim 1, wherein a distance between the target substrate and the second mirror is greater than 100 millimeters.

10. Objective optics for extreme ultra-violet light formed by an arrangement of mirrors, the objective optics comprising:

a first mirror which is arranged to receive and reflect the EUV light which is reflected from the target substrate,

a second mirror which is arranged to receive and reflect the EUV light which is reflected by the first mirror,

a third mirror which is arranged to receive and reflect the EUV light which is reflected by the second mirror, and

a fourth mirror which is arranged to receive and reflect the EUV light which is reflected by the third mirror,

wherein the numerical aperture of the objective optics is greater than 0.2.

.

11. The objective optics of claim 10, wherein the second mirror partially obscures the first mirror from the reflected EUV light.

12. The objective optics of claim 10, wherein the light reflected by the second mirror passes through an opening in the first mirror.

13. The objective optics of claim 10, wherein the first, second, third, and fourth mirrors are, respectively, concave, concave, convex and concave.

14. The objective optics of claim 10, wherein the first, second, third, and fourth mirrors are, respectively, concave, convex, concave and convex.

15. The objective optics of claim 10, wherein the first, second, third, and fourth mirrors are, respectively, concave, convex, concave, and concave

16. The objective optics of claim 10, wherein a field of view of the apparatus is at least greater than 5,000 square microns.

17. The objective optics of claim 10, wherein a distance between the target substrate and the second mirror is greater than 100 millimeters.

18. A method of projecting extreme-ultraviolet light reflected from a manufactured substrate to a sensor, the method comprising:

receiving and reflecting the EUV light which is reflected from the target substrate by a first mirror;

receiving and reflecting the EUV light which is reflected from the first mirror by a second mirror;

receiving and reflecting the EUV light which is reflected from the second mirror by a third mirror;

receiving and reflecting the EUV light which is reflected from the third mirror by a fourth mirror; and

detecting the EUV light which is reflected by the fourth mirror.

19. The method of claim 18, wherein the numerical aperture of the objective optics is greater than 0.2.

20. The method of claim 18, wherein the second mirror partially obscures the first mirror from the reflected EUV light.

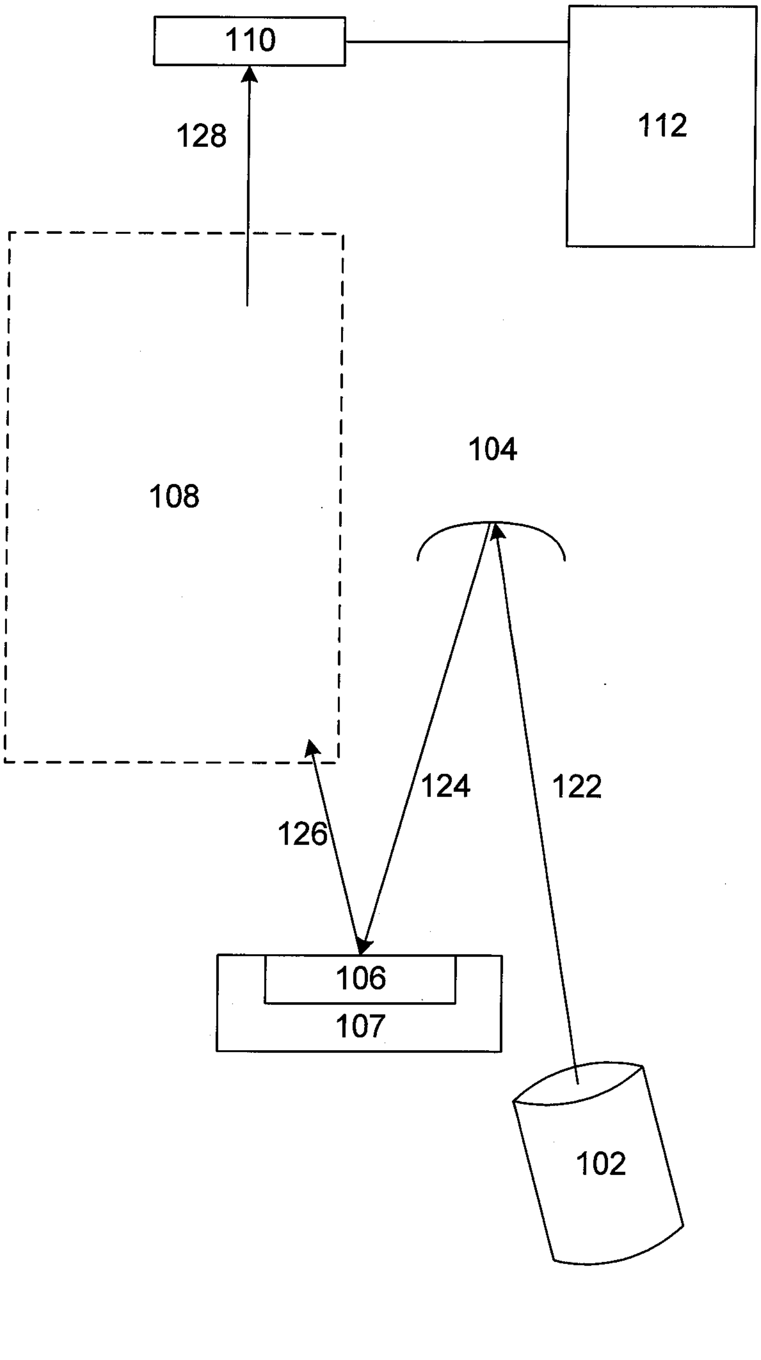

FIG. 1 100

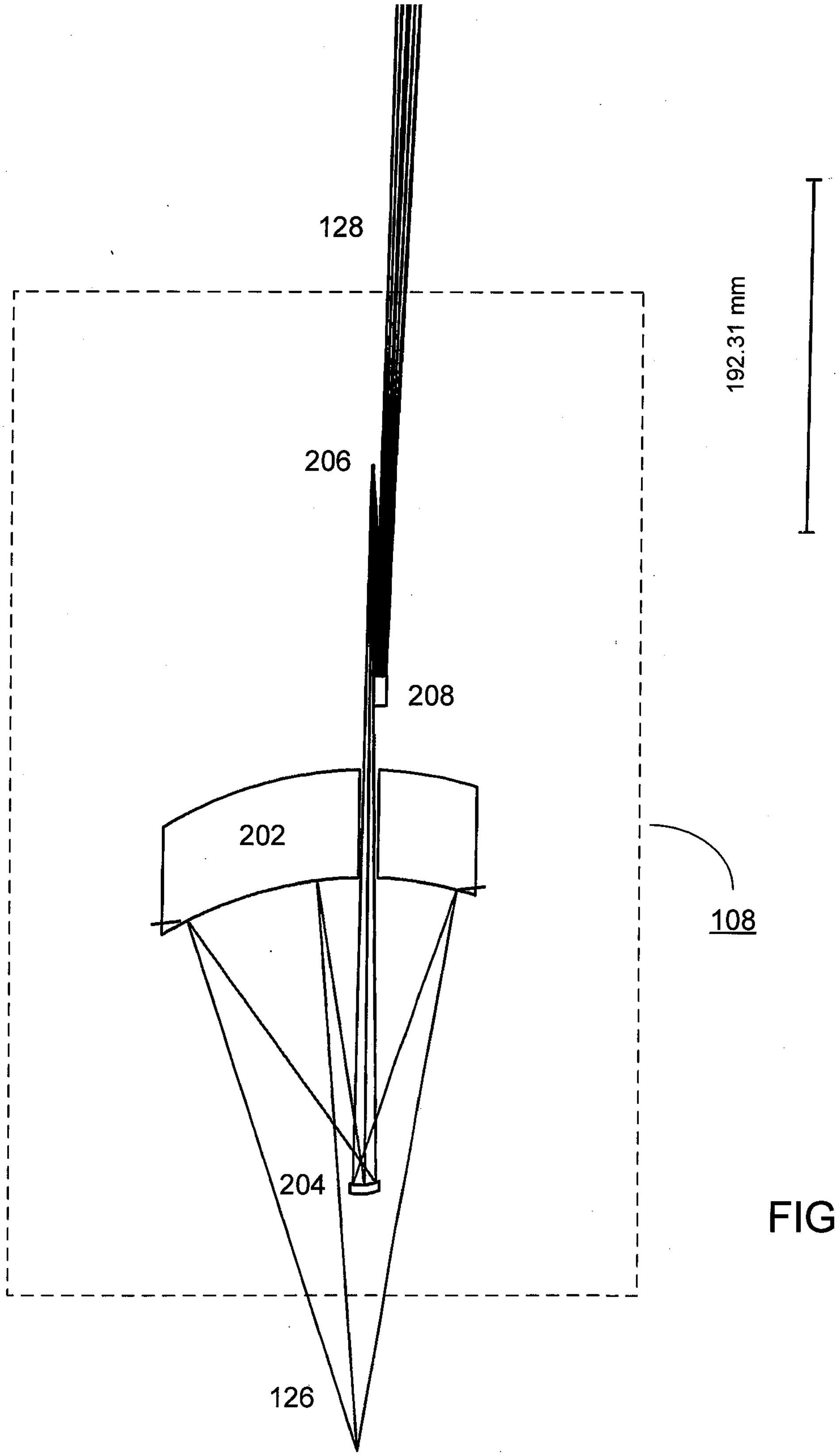

FIG. 2

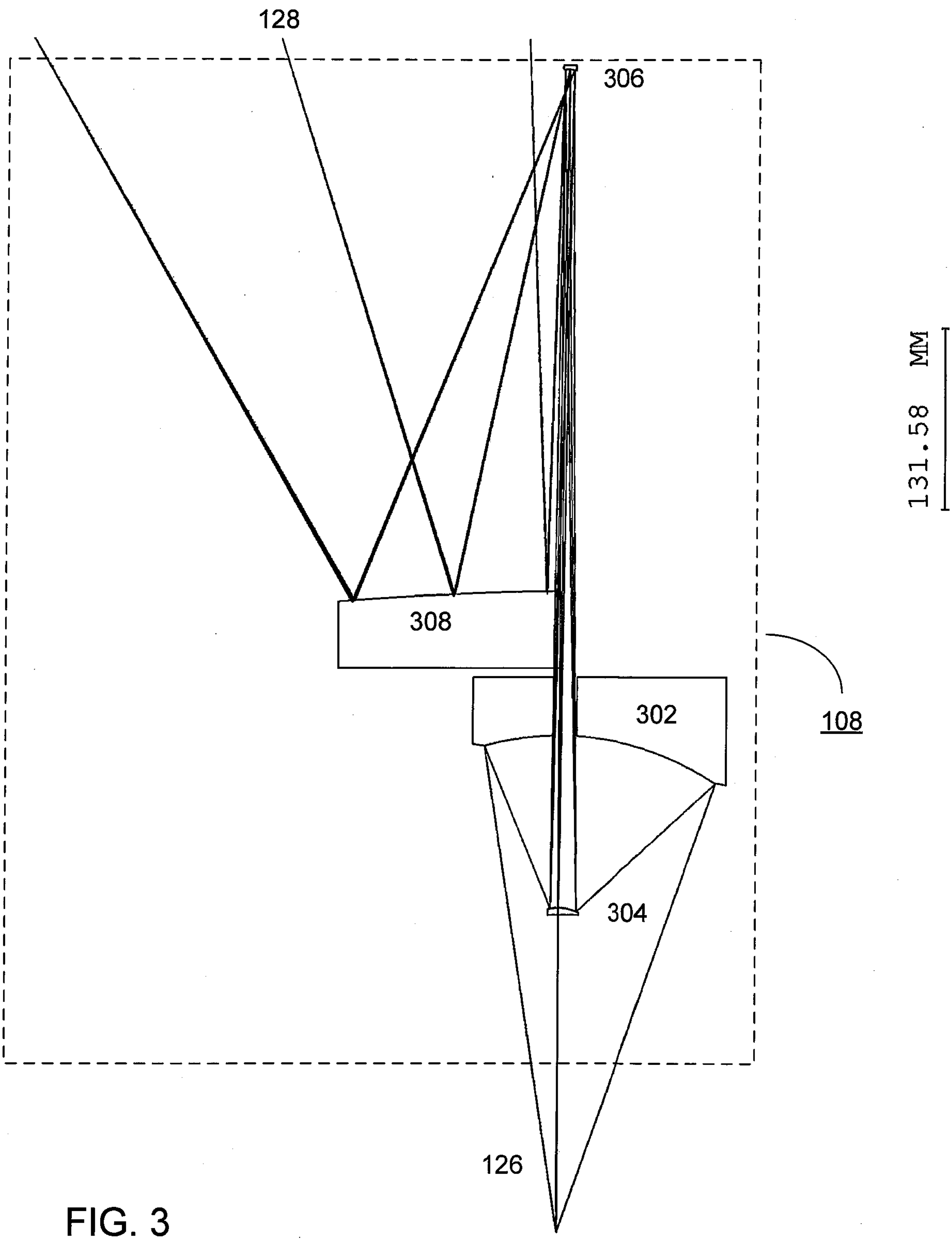

FIG. 3

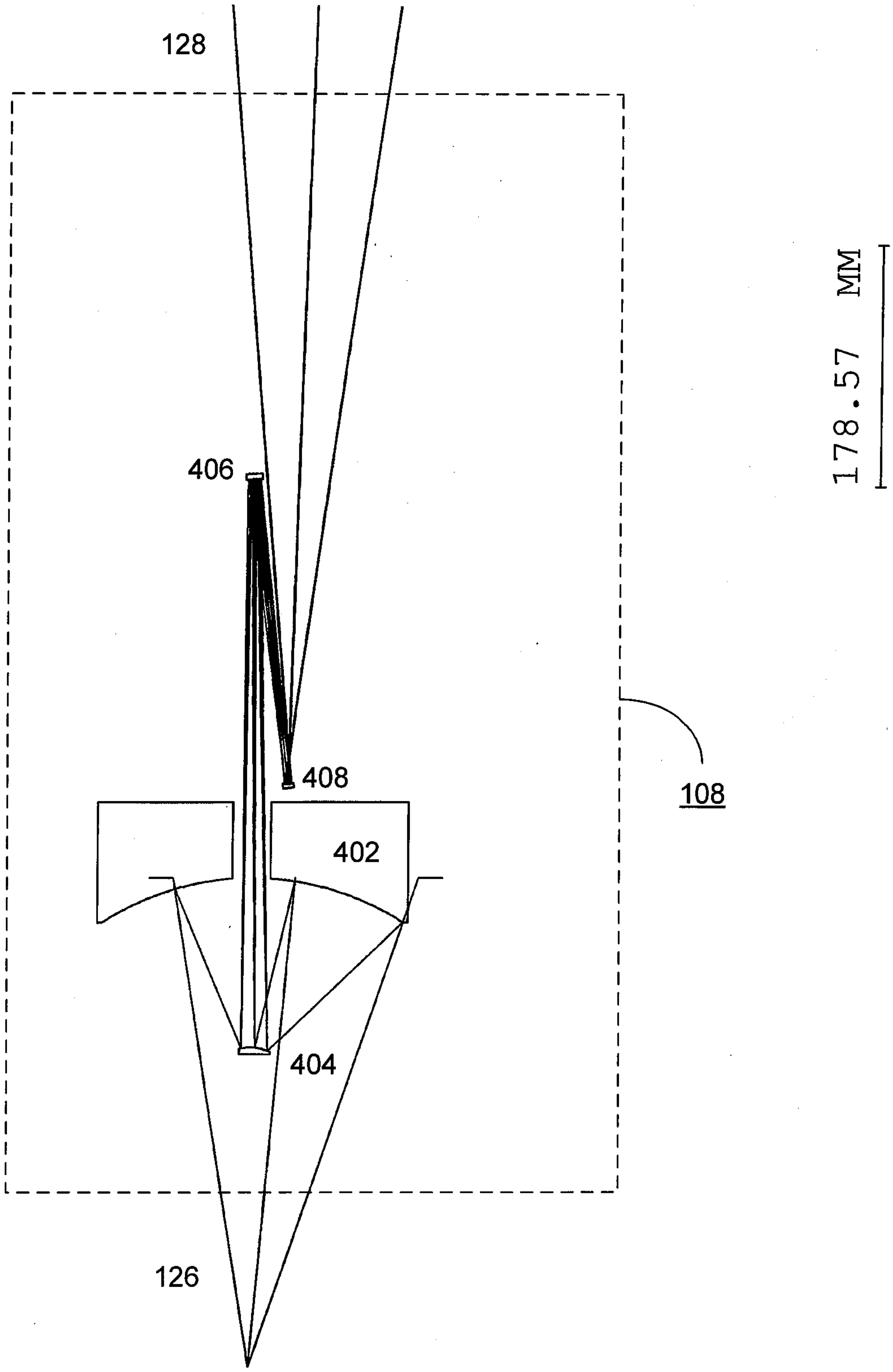

FIG. 4